

UC Berkeley

UC Berkeley Previously Published Works

Title

TBL10 is required for O-acetylation of pectic rhamnogalacturonan-I in *Arabidopsis thaliana*

Permalink

<https://escholarship.org/uc/item/26s206bv>

Journal

The Plant Journal, 96(4)

ISSN

0960-7412

Authors

Stranne, Maria
Ren, Yanfang
Fimognari, Lorenzo
[et al.](#)

Publication Date

2018-11-01

DOI

10.1111/tpj.14067

Peer reviewed

TBL10 is required for O-acetylation of pectic rhamnogalacturonan-I in *Arabidopsis thaliana*

Maria Stranne^{1,*}, Yanfang Ren^{2,3,†,*}, Lorenzo Fimognari¹, Devon Birdseye^{2,3}, Jingwei Yan^{2,3,4}, Muriel Bardor⁵, Jean-Claude Mollet⁵, Takanori Komatsu⁶, Jun Kikuchi⁶, Henrik V. Scheller^{2,3,7,*}  and Yumiko Sakuragi^{1,*} 

¹Copenhagen Plant Science Center, Department of Plant and Environmental Sciences, Faculty of Science, University of Copenhagen, Frederiksberg DK-1871, Denmark,

²Feedstocks Division, Joint Bioenergy Institute, Emeryville, CA 94608, USA,

³Environmental Genomics and Systems Biology Division, Lawrence Berkeley National Laboratory, Berkeley, CA 94720, USA,

⁴College of Life Sciences, Nanjing Agricultural University, Nanjing, Jiangsu 210095, China,

⁵Normandie Univ, UNIROUEN, Laboratoire Glyco-MEV, 76000 Rouen, France,

⁶RIKEN Center for Sustainable Resource Science, Yokohama, Kanagawa 230-0045, Japan, and

⁷Department of Plant and Microbial Biology, University of California, Berkeley, CA 94720, USA

Received 13 June 2018; accepted 6 August 2018; published online 17 August 2018.

*For correspondence (e-mails ysa@plen.ku.dk; hscheller@lbl.gov).

†School of Environmental and Safety Engineering, Changzhou University, Changzhou, Jiangsu 213164, China

‡These authors contributed equally to the work.

SUMMARY

O-Acetylated pectins are abundant in the primary cell wall of plants and growing evidence suggests they have important roles in plant cell growth and interaction with the environment. Despite their importance, genes required for O-acetylation of pectins are still largely unknown. In this study, we showed that *TRICHOME BIREFRINGENCE LIKE 10* (*AT3G06080*) is involved in O-acetylation of pectins in *Arabidopsis* (*Arabidopsis thaliana*). The activity of the *TBL10* promoter was strong in tissues where pectins are highly abundant (e.g. leaves). Two homozygous knock-out mutants of *Arabidopsis*, *tbl10-1* and *tbl10-2*, were isolated and shown to exhibit reduced levels of wall-bound acetyl esters, equivalent of ~50% of the wild-type level in pectin-enriched fractions derived from leaves. Further fractionation revealed that the degree of acetylation of the pectin rhamnogalacturonan-I (RG-I) was reduced in the *tbl10* mutant compared to the wild type, whereas the pectin homogalacturonan (HG) was unaffected. The degrees of acetylation in hemicelluloses (i.e. xyloglucan, xylan and mannan) were indistinguishable between the *tbl10* mutants and the wild type. The mutant plants contained normal trichomes in leaves and exhibited a similar level of susceptibility to the phytopathogenic microorganisms *Pseudomonas syringae* pv. tomato DC3000 and *Botrytis cinerea*; while they displayed enhanced tolerance to drought. These results indicate that TBL10 is required for O-acetylation of RG-I, possibly as an acetyltransferase, and suggest that O-acetylated RG-I plays a role in abiotic stress responses in *Arabidopsis*.

Keywords: O-acetylation, pectin, rhamnogalacturonan I, the cell wall, *Arabidopsis thaliana*.

INTRODUCTION

In plants, the cell wall is composed of a dynamic network of polysaccharides, proteins, and lignin. This network plays a myriad of roles in plant development, growth, and responses to biotic and abiotic environmental stimuli (Carpita, 2015). Polysaccharides are the main components of the plant cell wall and are divided into three main classes: cellulose, hemicelluloses, and pectins. Cellulose microfibrils are bundles of linear β -(1,4)-linked glucans and provide load-bearing networks that are cross-linked via non-covalent bonds by hemicelluloses and pectins (Carpita, 2015).

Hemicelluloses contain backbones of β -(1,4)-linked neutral sugars including glucose (Glc), xylose (Xyl) or mannose (Man), which can be further decorated with mono- or oligo-saccharide side chains. In the primary cell wall of dicots and conifers, the major hemicellulose is xyloglucan (XyG), although glucuronarabinoxylans and mannans are also found albeit to a lesser extent (Scheller and Ulvskov, 2010). In contrast to hemicelluloses and cellulose, pectins contain backbones rich in galacturonic acid (GalA). Pectins are classified into four major types: homogalacturonan

(HG), xylogalacturonan, rhamnogalacturonan (RG)-I and RG-II. HG is a homomeric polymer consisting of α -(1,4)-linked D-GalA with methyl- and acetyl-substitutions on C6 and O2/O3, respectively. The backbone of RG-I consists of the repeating disaccharide, 4)- α -D-GalA- α -(1,2)-L-Rha-(1 (wherein Rha indicates rhamnose), which is substituted with galactan, arabinan, and/or arabinogalactan side chains on the Rha residues (Mohnen, 2008; Atmodjo *et al.*, 2013). Pectins are highly abundant in the primary cell wall surrounding cells in growing tissues and play critical roles in cell-to-cell adhesion, cell expansion, organ development and response to microbial pathogens (Ridley *et al.*, 2001).

One of the notable structural features of pectins and hemicelluloses is the presence of *O*-acetyl esterification. Concerning pectins, many GalA residues in the backbones of HG and RG-I are *O*-acetylated at the positions O2 and/or O3 (Lerouge *et al.*, 1993; Ishii, 1997; Perrone *et al.*, 2002). RG-II can be acetylated in the B side chain (Whitcombe *et al.*, 1995; Pabst *et al.*, 2013). The degree of acetylation (DA) of the pectic polymers ranges from 40 to 85% depending on tissues (Liners *et al.*, 1994; Ishii, 1997; Perrone *et al.*, 2002). Concerning hemicelluloses, xylans are acetylated in the Xyl backbone with a DA of up to 50% (Ishii, 1991; Gonçalves *et al.*, 2008; Xiong *et al.*, 2013; Busse-Wicher *et al.*, 2014). A similar DA was also reported for mannan (Manna and McAnalley, 1993; Lundqvist *et al.*, 2002; Nunes *et al.*, 2005; Xiong *et al.*, 2013). In XyG, the Gal residues on the side chains can be acetylated (Gille *et al.*, 2011), while *O*-acetylation of the backbone Glc residues has also been reported (Sims *et al.*, 1996; York *et al.*, 1996). *In vitro*, *O*-acetylation affects the gelling capability of pectin (Vriesmann and Petkowicz, 2013). *In vivo*, *O*-acetylation of pectin has been reported to affect the stiffness of tissues in potato tubers and Arabidopsis, pathogen resistance in Arabidopsis and *Brachypodium distachyon*, and the assembly of the cell wall and the cuticle layer in Arabidopsis (Gou *et al.*, 2012; Orfila *et al.*, 2012; Pogorelko *et al.*, 2013; Nafisi *et al.*, 2015).

O-Acetylation of pectins and hemicelluloses requires acetyl-CoA in the cytosol as the acetyl-donor (Pauly and Scheller, 2000), and the acetyl moiety is thought to be transported across the membrane in the Golgi apparatus and subsequently transferred to substrate polysaccharides by acetyltransferases. Genetic evidence suggests that a family of proteins, reduced wall acetylations (RWAs), function as acetyl-transporters (Lee *et al.*, 2011; Manabe *et al.*, 2011, 2013). There are four *RWA* genes in the Arabidopsis genome, and knock-out mutants in *RWA2* resulted in partial losses of *O*-acetylation in both pectins and hemicelluloses by approximately 20% of the wild-type level; furthermore combinatorial knock-out mutants among the four genes dramatically reduced the level of cell wall acetylation (Lee *et al.*, 2011; Manabe *et al.*, 2011, 2013). The *rwa2* knock-out mutants exhibited pleiotropic phenotypes

in leaves, including collapsed trichomes, increased surface permeability, and enhanced resistance to the necrotrophic fungal pathogen *Botrytis cinerea* (Manabe *et al.*, 2011; Nafisi *et al.*, 2015). Regarding the transfer of the acetyl group onto polysaccharides, this step is thought to be catalyzed by proteins belonging to the trichome birefringence like family (TBL), and this notion has been augmented by the finding that heterologously expressed TBL29/ESKIMO1 transferred acetyl groups from acetyl-CoA to xylan oligosaccharides (Gille *et al.*, 2011; Lee *et al.*, 2011; Yuan *et al.*, 2013; Urbanowicz *et al.*, 2014). An additional protein plays a role in *O*-acetylation of XyG, as recent evidence suggested that altered xyloglucan 9 (AXY9) is involved in mediating the transfer of the acetyl group from RWAs to TBLs, while this protein is not required for pectin *O*-acetylation (Schultink *et al.*, 2015).

There are 46 TBLs encoded in the Arabidopsis genome (Bischoff *et al.*, 2010). For the ease of description, Figure S1 presents a phylogenetic tree of the TBLs showing distinct clusters and they are labeled as Cluster I through V. trichome birefringence (TBR), the first reported member in TBLs, is found in Cluster I. The *tbr* mutant was found to have a lower level of pectin esterification and also a reduced amount of crystalline cellulose as compared to the wild type (Potikha and Delmer, 1995; Bischoff *et al.*, 2010). Recently, it was shown that the *tbr* mutant has an increased level of methylesterification and a reduced level of *O*-acetylation in pectins, although it is yet unclear which type(s) of pectin was affected (Sinclair *et al.*, 2017). TBL44/powdery mildew resistant 5 (PMR5) is found in Cluster II and the *tbl44* mutant also exhibited a lower level of pectin esterification as compared to wild-type cell walls (Vogel *et al.*, 2004). Again, it is not yet clear whether the decrease is due to methyl- or acetyl-esterification. No TBL protein belonging to Cluster III or its corresponding mutants has been described so far. Cluster IV contains TBL3, TBL29, TBL31, TBL32, TBL33, TBL34 and TBL35, which have been shown to be involved in acetylation of xylan, and mannan in some cases (Lee *et al.*, 2011; Yuan *et al.*, 2013, 2016a,b,c; Urbanowicz *et al.*, 2014). Notably, a homolog of Arabidopsis TBL34 in rice (OsTBL1), was shown to transfer the acetyl group from acetyl-CoA to xylooligosaccharides (Gao *et al.*, 2017). TBL27/AXY4 and TBL22/AXY4L are found in Cluster V, and both *tbl27* and *tbl22* contain reduced levels of xyloglucan *O*-acetylation (Gille *et al.*, 2011). Additionally, TBL25 and TBL26 were implicated in acetylation of mannan (Gille *et al.*, 2011). Hence, it is likely that TBLs belonging to Cluster IV and V are involved in *O*-acetylation of hemicelluloses while TBLs belonging to one or more of the remaining clusters function in *O*-acetylation of pectins.

In this study, we investigated TBL10 (AT3G06080), belonging to Cluster I and exhibiting a 29% amino acid sequence identity to TBR. Our results show that TBL10 is involved in *O*-acetylation of RG-I, *tbl10* mutants display the

wild-type level of susceptibility to *P. syringae* and *B. cinerea*, while they are more resistant to drought stress.

RESULTS

Isolation of T-DNA insertion mutants in *TBL10*

TBL10 is annotated to contain 4 exons and encodes a protein consisting of 444 amino acid residues (<http://www.a.rabidopsis.org/>). The deduced amino acid sequence of *TBL10* contained a single membrane-spanning region in the *N*-terminus (<http://aramemnon.botanik.uni-koeln.de/>; Schwacke *et al.*, 2003), which is likely to serve as a signal sequence and membrane anchor based on analysis by SignalP4.0 (<http://www.cbs.dtu.dk/services/SignalP/>; Petersen *et al.*, 2011). Several notable conserved domains and motifs among TBLs (Bischoff *et al.*, 2010) were found within *TBL10*, including the PMR5 *N*-terminal domain (Pfam13839) between the amino acid positions 102 and 154, GDSL/SGH-like acylesterase family domain (Pfam14416) between the amino acid positions 144 and 444, which also includes the conserved DUF231 domain (the amino acid positions 278 and 444), and the Gly-Asp-Ser motif (the amino acid positions 176–178) and the Asp-X-X-His (the amino acid positions 424–427, wherein X indicates any amino acid residues).

Two T-DNA insertion lines of *Arabidopsis* ecotype Columbia-0 with T-DNA insertion in the 1st and the 3rd exons of *TBL10* were isolated and were designated as *tbl10-1* (SALK_005890C) and *tbl10-2* (SALK_011296), respectively (Figure 1a). The presence of the T-DNA inserts in *TBL10* was confirmed by PCR (Figure 1b). Both lines were shown to possess the T-DNA insert in *TBL10* while the wild-type allele was non-detectable. In addition, RT-PCR analysis showed that the *TBL10* transcript was detectable both in the leaves and stems in the wild type, while it was not detectable in the mutants (Figure 1c). These results confirmed that *tbl10-1* and *tbl10-2* are homozygous knock-out mutants. The *tbl10* mutant plants grew similarly to the wild type without notable changes in morphologies under the conditions tested. Representative images of rosettes and mature plants are shown in Figure 1(d).

TBL10 is expressed in leaves and roots

To further investigate the tissue-wide expression pattern of *TBL10*, the 1800-bp sequence immediately upstream of the *TBL10* start codon was fused with the β -glucuronidase (GUS) gene and wild-type plants were transformed with the fusion construct. Analysis of five independent transformants in the T2 generation showed that the GUS activity was the strongest in leaves and roots, while significantly less activity was observed in stems (Figure 2a). The promoter was active in rosette leaves, cauline leaves, roots, flowers, and seedlings, with notable activity in the vascular system (Figure 2a,b,e,g,h). The activity was also observed

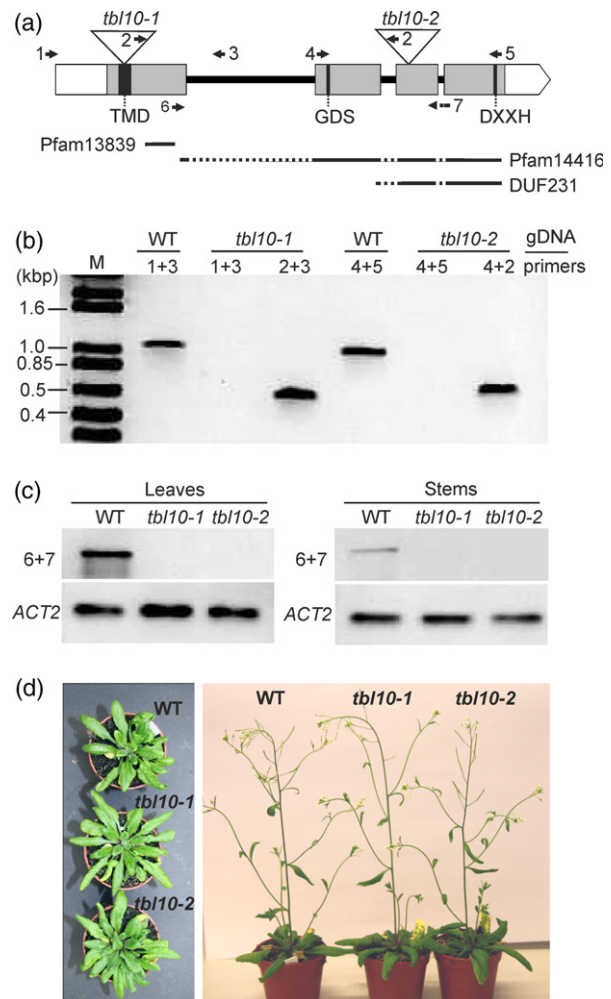
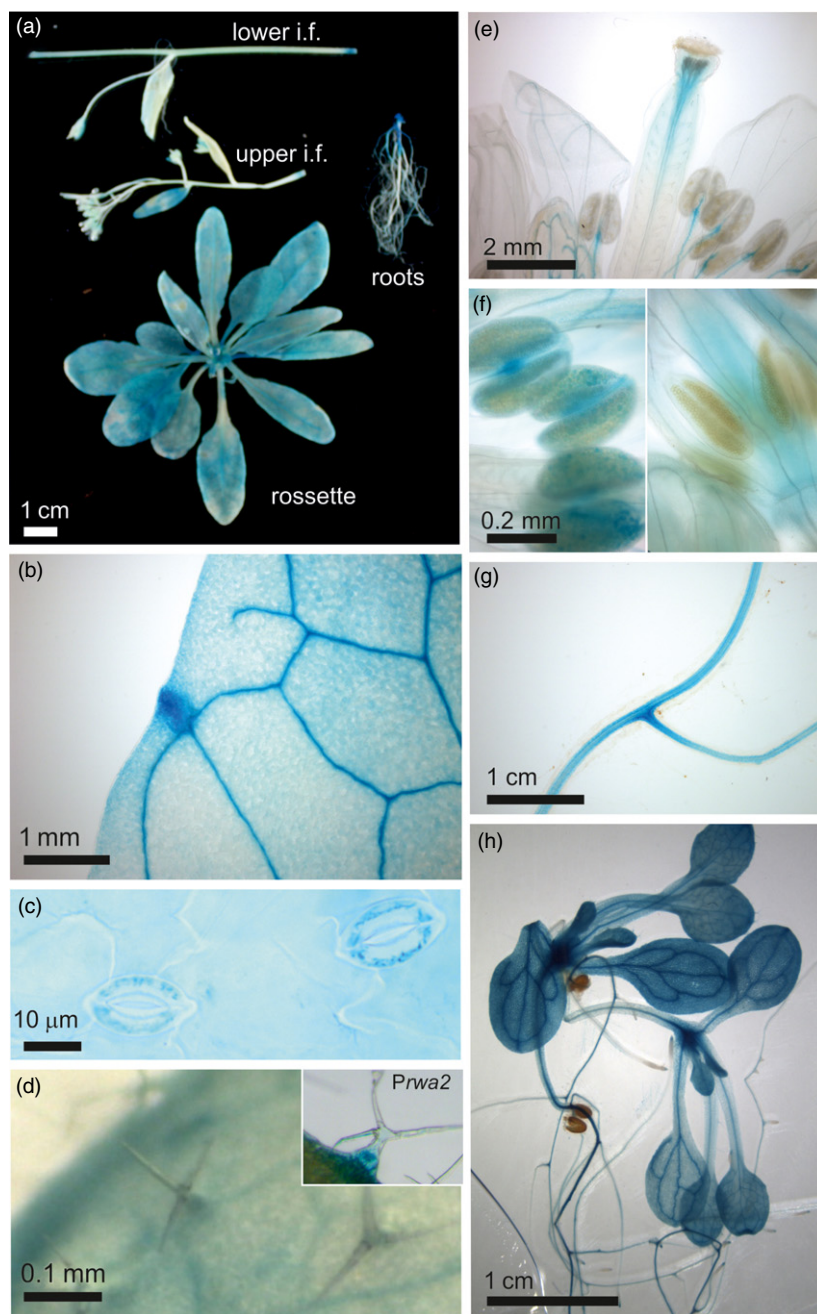


Figure 1. Isolation of homozygous *tbl10* mutants of *Arabidopsis*. (a). Gene model of *TBL10* showing T-DNA insertional sites for *tbl10-1* and *tbl10-2* and primer binding sites. The presence of a transmembrane domain (TMD) and motifs (GDSL and DXXH) conserved among TBL family proteins are also indicated. Nucleotide regions encoding conserved domains (Pfam13839, the PMR5 *N*-terminal domain; Pfam14416, GDSL/SGH-like acylesterase family domain; DUF231) are marked by solid bars, wherein dotted areas indicate the exons. (b) Genotype analysis by PCR using target specific primers as shown in panel (a). Genomic DNA (gDNA) isolated from the indicated plants was used as the template. (c) Analysis of the presence of the *TBL10* transcript in leaves and stems. Primer 6 and 7 were used to detect the *TBL10* transcript, as shown in panel (a). Primer 7 spanned exons 3 and 4. *ACTIN2* (*ACT2*) was used as a reference gene. Total RNAs were isolated from the respective genotypes, normalized to the same amount, and used as the template. (d) Representative images of the wild-type and the *tbl10* mutant plants after 8 weeks (left) and 12 weeks (right). [Colour figure can be viewed at wileyonlinelibrary.com].

in stomata in rosette leaves (Figure 2c), but not in trichomes (Figure 2d). In flowers, the GUS activity was mainly observed in matured flowers (developmental stage of 16 according Alvarez-Buylla *et al.*, 2010), particularly in the vasculature and pollen (Figure 2e,f). Following a saturating staining, stems also showed the GUS activity, although the intensity was markedly weaker as compared

Figure 2. The *TBL10* promoter::*GUS* activity in *Arabidopsis*.

T2 generations of transgenic plants bearing the *TBL10*-promoter::*GUS* reporter gene fusion construct were analyzed. (a) Mature plant (11-week-old plant). (b–d) Close-up images of a rosette leaf showing a marked staining in the vasculature (b) and stomata (c), and the absence of notable staining in trichomes (d). For comparison, staining of a trichome in an *RWA2* promoter::*GUS* plant (Prwa2; Nafisi *et al.*, 2015) is shown in the insert. (e) Flowers. (f) Close-up images of anthers in the flower developmental stages of 16 (left) and 15 (right). (g) Roots. (h) Seedlings. Plant materials shown in panels (a) through (g) were grown in soil, while the seedlings shown in panel (h) were grown in ½ Murashige-Skoog media containing 1% (w/v) sucrose and 1% (w/v) agar. All plants were grown in the diurnal cycle of 12-h light and 12-h darkness. [Colour figure can be viewed at wileyonlinelibrary.com].



to the leaves (Figure S2a). *In silico* gene expression analysis of publicly available *Arabidopsis* microarray datasets using *Arabidopsis* eFP Browser (Winter *et al.*, 2007) confirmed high transcript levels of *TBL10* in leaves (cauline leaves, adult and juvenile leaves, cotyledons) (Figure S2b).

The *tbl10* mutants have reduced amount of *O*-acetylation in pectins

The content of wall-bound acetyl esters was determined in leaves and stems of the wild type, *tbl10-1* and *tbl10-2*. Total cell walls were extracted by alcohol precipitation and

alcohol insoluble residues (AIR) were treated with α -amylase to remove starch. De-starched AIR was subjected to a treatment with NaOH and the amount of acetic acid due to the alkali-labile acetyl esters was quantified colorimetrically using an enzyme-coupled assay. In comparing the acetic acid levels in leaves, significant reductions, to 56 and 65% of the wild-type level, were observed for *tbl10-1* and *tbl10-2*, respectively (Figure 3a). In contrast, when the acetic acid contents were compared in the stems, no obvious difference was observed between the genotypes (Figure 3b).

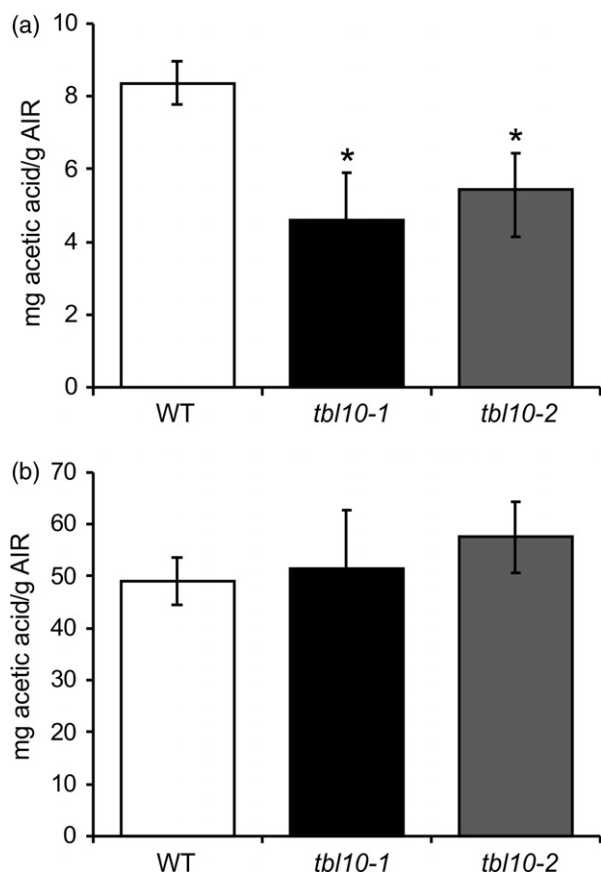


Figure 3. Acetyl ester contents in cell walls isolated from the wild type, *tb110-1* and *tb110-2* mutants of Arabidopsis.

Destarched AIR derived from leaves (a) and stems (b) were analyzed. Ten milligrams of destarched AIR was saponified with NaOH and the acetic acid content was determined. Three independent biological samples were analyzed for each genotype. Error bars indicate standard deviations. Asterisks (*) indicate significant difference from the wild type as determined by Student's *t*-test ($P < 0.05$).

Because the leaves of the *tb110* mutants showed a large change in the content of alkali-labile acetyl esters, monosaccharide compositions of the cell wall polysaccharides were determined in de-starched AIR derived from leaves. With an exception of minor changes observed for the *tb110-2*, no significant difference was observed between the wild type and the *tb110* mutants as shown in Table 1.

Next, de-starched AIR obtained from leaves and stems of the wild type and the *tb110* mutants were fractionated into pectin-enriched and pectin-depleted fractions after a treatment with pectin methyl esterase (PME) and *endo*-polygalacturonase (ePG) followed by centrifugation. The supernatants and the pellets represented the pectin-enriched and the pectin-depleted fractions, respectively. The monosaccharide compositions of the respective fractions from the wild type and the *tb110* mutants were indistinguishable (Figure S3). As expected with the enzymatic treatment employed, the pectin-enriched fractions had a

Table 1 Monosaccharide composition of AIR isolated from leaves of the wild type and the *tb110* mutants of Arabidopsis

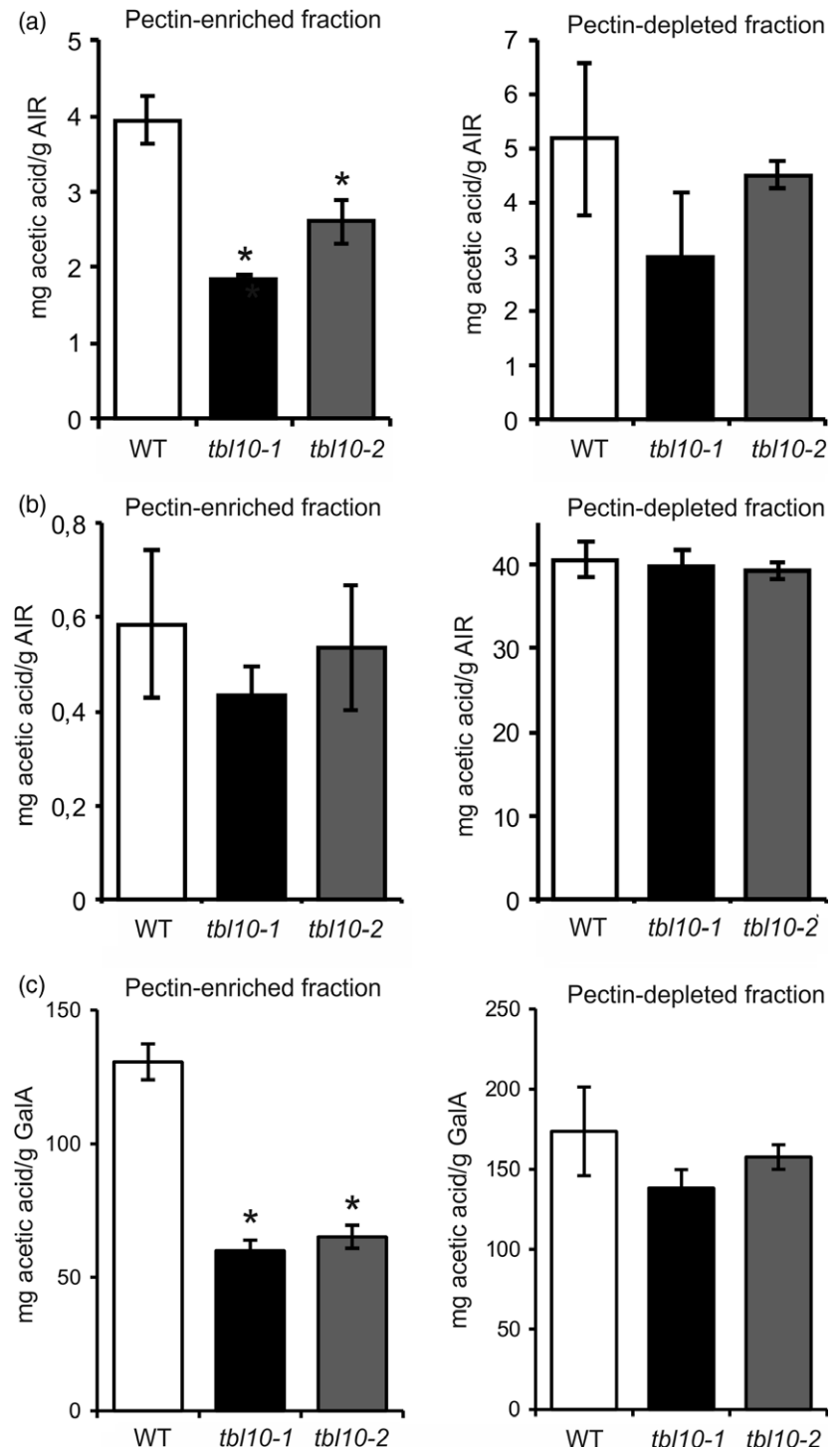
Monosaccharide	Wild type	<i>tb110-1</i>	<i>tb110-2</i>
Fuc	1.81 ± 0.05	2.06 ± 0.11	1.94 ± 0.07
Ara	15.74 ± 1.09	16.05 ± 1.06	15.57 ± 0.92
Rha	9.73 ± 0.22	11.32 ± 0.51	10.16 ± 0.23
Gal	19.10 ± 1.07	18.34 ± 0.87	17.48 ± 1.19
Glc	6.50 ± 1.16	4.98 ± 0.52	4.84 ± 0.32
Xyl	15.49 ± 1.96	16.23 ± 0.60	15.77 ± 0.34
Man	2.52 ± 0.52	2.74 ± 0.23	2.74 ± 0.17
GalA	27.95 ± 0.38	27.22 ± 2.42	30.32 ± 1.96
GlcA	1.16 ± 0.09	1.07 ± 0.22	1.18 ± 0.36

After hydrolysis of the AIR, released sugars were analyzed by HPAEC-PAD. The values are expressed as mol% and as average of three biological replicates ±SD. None of the sugars showed statistical difference between wild type and mutants (Student's *t*-test with Bonferroni correction, $P > 0.05$). Ara, arabinose; GlcA, glucuronic acid. Abbreviations for the other monosaccharides are found in the text.

composition consistent with them being almost exclusively composed of pectin, while the pectin-depleted fractions contained significant amounts of GalA, indicating that the enzyme treatment did not completely solubilize pectin (Figure S3). When the levels of alkali-labile acetyl esters were compared for pectin-enriched fractions derived from leaves, the *tb110* mutants showed a significant reduction compared to the wild type. On the other hand, pectin-depleted fractions showed a trend toward reductions, although this was not statistically significant (Figure 4a). Given that the pectin-depleted fractions still contained pectin, the observed trend likely reflects reduced acetylation in the remaining pectin. The same analysis was performed using fractionated de-starched AIR derived from stems (Figure 4b). The small amount of pectin in the stem samples contributed little to the total amount of acetyl esters, and although the pattern resembled that of pectin-enriched samples from leaves, the differences were not significant. The pectin-depleted samples from the stems had a large amount of acetyl esters, as expected in samples with a high content of acetylated xylan, but no significant difference was observed (Figure 4b). When the amounts of alkali-labile acetyl esters in leaves were normalized by the amount of GalA, marked reductions (~50%) in the levels of acetyl ester were found in the pectin-enriched fractions derived from *tb110* mutants compared to the wild type (Figure 4c). Again, there was a trend towards reduction in the pectin-depleted fractions from the mutants. Taken together, these results indicate that the knockout mutations in *TBL10* impairs acetylation of pectins.

In order to probe which pectin polymers were affected by the *tb110* mutation, RG-I and HG from the wild type and *tb110-1* were isolated after a treatment of the AIR with PME and ePG as previously described (Stonebloom *et al.*, 2016) and the fractions corresponding to RG-I and HG were

Figure 4. Acetyl ester contents in pectin-enriched and pectin-depleted fractions obtained from the *Arabidopsis* wild-type and *tbl10* mutant cell walls. Destarched AIR from leaves (a) and stems (b) was treated with ePG and PME and separated into the pectin-enriched and pectin-depleted fractions. Each fraction was saponified and the acetic acid contents were determined. (c) Normalized acetic acid contents by the GalA contents in leaves. The acetic acid contents in the pectin-enriched and pectin-depleted fractions obtained from the leaf material were normalized by the GalA content in the same fractions. Error bars indicate standard deviations of three to five independent biological replicates. Asterisks (*) indicate significant differences from the wild type as determined by Student's *t*-test ($P < 0.05$).



analyzed for alkali-labile acetyl ester content. In the isolated RG-I, the molar ratio between acetyl ester and GalA was markedly reduced in *tbl10-1* compared to the wild type (Figure 5a). In contrast, the molar ratio between acetyl groups and GalA was indistinguishable between the wild type and the mutant in the HG fractions (Figure 5b). These results indicate that *TBL10* is required for the *O*-acetylation of RG-I.

Acetylation of hemicelluloses are not affected in the *tbl10* mutants

The pectin-depleted fractions from leaves showed a trend towards lower levels of acetyl esters in the mutants. While this could be explained by residual pectin in the fractions, we wanted to directly assess if any hemicelluloses were

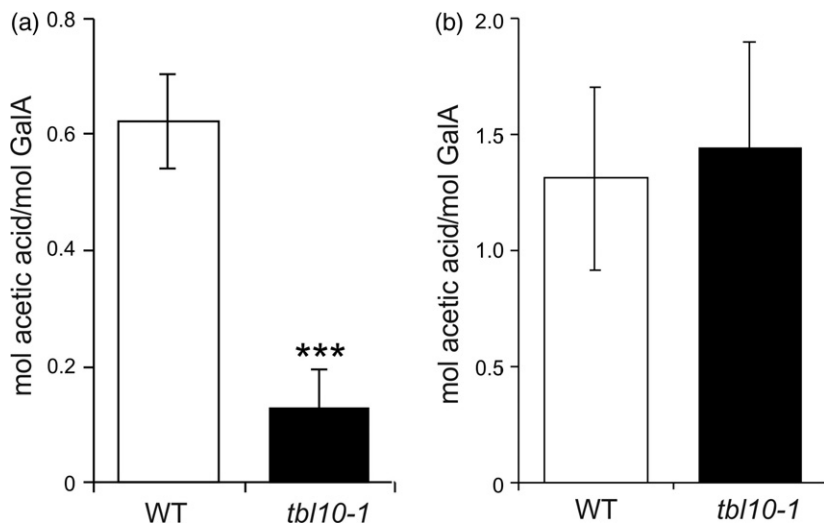


Figure 5. Degree of acetylation in the RG-I and HG isolated from the wild type and *tbl10-1* mutant of Arabidopsis.

(a) Isolated RG-I. (b) Isolated HG. RG-I and HG were isolated after treatment with ePG and PME followed by size exclusion chromatography. The acetic acid contents were normalized by the GalA content in the same fractions. Error bars indicate standard deviations of four independent biological replicates. Asterisks (***) indicate significant difference from the wild type as determined by Student's *t*-test ($P < 0.001$).

altered in their acetylation as well. This possibility was first tested by analyzing the structure of XyG, the most abundant hemicellulose in leaves, by comparing the oligosaccharide profiles after enzymatic digestion followed by a matrix-assisted-laser desorption-ionization-time-of-flight mass spectrometry (MALDI-TOF MS) (Figure 6). In most eudicots, the glucan backbone of XyG can be substituted with Xyl, Gal-Xyl, and Fuc-Gal-Xyl (where Fuc is fucose) side chains corresponding to notations of X, L and F, respectively (Fry *et al.*, 1993). The wild type and the *tbl10* mutants showed the same distribution patterns of the acetylated and non-acetylated XyG motifs (Figure 6a). Moreover, the relative abundance of acetylated XyG motifs were also unaltered (Figure 6b). These results indicate that TBL10 does not affect XyG *O*-acetylation (Figure 6).

Mannans and xylans are dominant hemicelluloses in stems. Because the TBL10 promoter activity in stems was notably low and also no significant impact in the level of acetylation was observed in the stem of *tbl10* mutants, we speculated that TBL10 is not involved in *O*-acetylation of these hemicelluloses. Heteronuclear single quantum coherence experiments (HSQC) of two dimensional nuclear magnetic resonance spectrometry (2D-NMR), as previously described (Gille *et al.*, 2011; Cheng *et al.*, 2013), revealed that the abundances of acetylated mannan and xylan are largely unaffected in the *tbl10* mutant as compared to the wild type (Figure S5, Method S1). Consistent with these results, no difference in the morphological appearance of the tissues including xylem and lignin staining was observed in the stem sections of the wild type and the *tbl10* mutants (Figure S6, Method S2).

The *tbl10* mutants exhibit the wild-type-level of susceptibility towards biotic stress

Previously, ectopic overexpression of an RG-I acetyltransferase (RGAE) from *Aspergillus nidulans* in Arabidopsis has

led to increased resistance against the necrotrophic fungal pathogen *B. cinerea* (Pogorelko *et al.*, 2013). Therefore, we tested if reduced acetylation of RG-I in *tbl10* mutants might affect susceptibility to *B. cinerea*. Upon infection by *B. cinerea*, *tbl10-1* and *tbl10-2* showed lesion sizes that were similar to those in the wild type, while *rwa2-3*, used here as a control, showed markedly reduced lesion sizes as previously shown (Manabe *et al.*, 2011; Nafisi *et al.*, 2015) (Figure 7a). Likewise, no difference between the *tbl10* mutants and the wild type was seen when infected with *Pseudomonas syringae* pv. Tomato DC3000 (Figure 7b). Hence, unlike RWA2, TBL10 does not seem to have any impact for biotic stress response under the conditions tested.

Next, the integrity of trichomes in leaves was inspected. Trichomes of the *tbr* mutant contain reduced amount of crystalline cellulose, lack birefringence upon UV illumination, and are fragile or collapsed (Potikha and Delmer, 1995; Bischoff *et al.*, 2010; Suo *et al.*, 2013). Similarly to the *tbr* mutant, we have previously reported that *rwa2* mutants also contain collapsed trichomes, albeit without notable impact on trichome birefringence (Nafisi *et al.*, 2015). The staining of leaves with toluidine blue was employed as a diagnostic tool to detect compromised trichomes because this cationic dye can penetrate through the cuticle layer of collapsed trichomes but not of intact trichomes (Tanaka *et al.*, 2004; Nafisi *et al.*, 2015). The trichomes of the *tbl10* mutants appeared normal and did not stain with toluidine blue (Figure 7c,d), whereas those of the *rwa2-3* mutant exhibited collapsed and stained trichomes by toluidine blue (Figure 7c,d). Lastly, water loss of detached leaves was analyzed as collapsed trichomes can increase the surface transpiration as previously observed for *rwa2-3* (Nafisi *et al.*, 2015). The rate of weight loss was indistinguishable between the wild type and the *tbl10* mutants, while *rwa2-3* exhibited an enhanced rate of

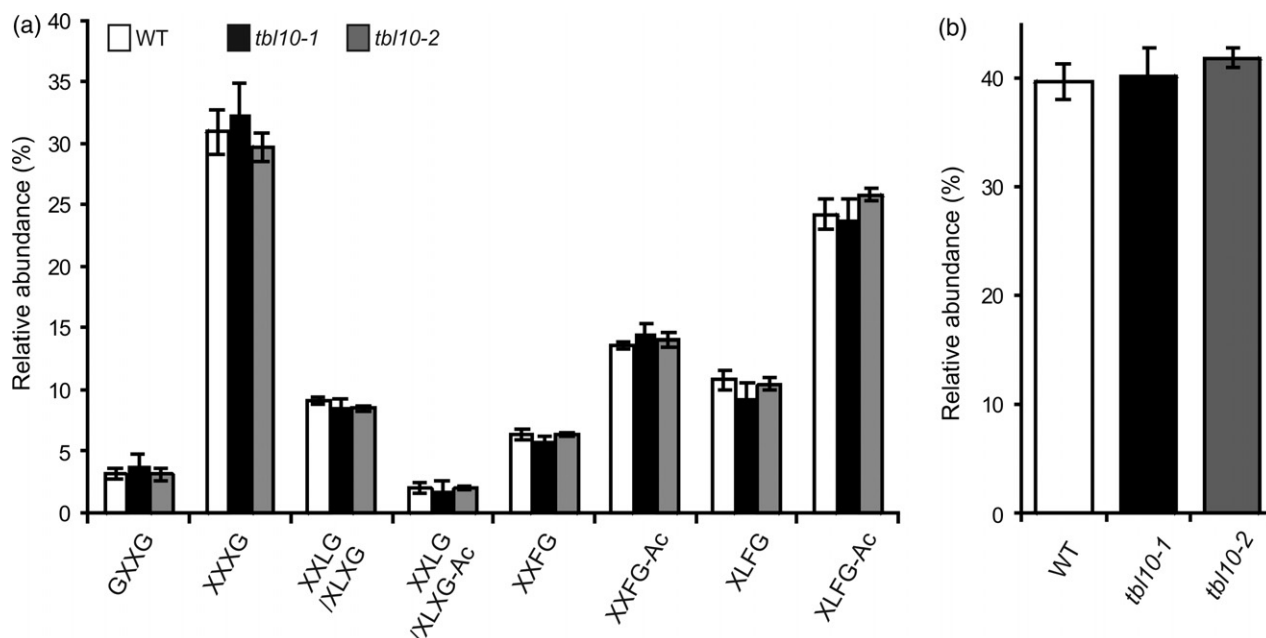


Figure 6. Xyloglucan (XyG) oligosaccharide profiling of the *Arabidopsis* wild-type, *tbl10-1* and *tbl10-2* cell walls by MALDI-TOF MS. (a) Relative abundance of XyG oligosaccharides released after *endo*-glucanase treatment. The nomenclature follows the one letter code proposed by Fry *et al.* (1993). Ac indicates the presence of an *O*-acetyl group. (b) Relative abundance of total *O*-acetylated XyG oligosaccharides. Data are the mean \pm SD from four independent biological replicates. No statistically significant difference was observed as assessed by Student's *t*-test ($P > 0.05$).

water loss under the same conditions (Figure 7e). Hence, unlike *rwa2* and *tbr* mutants, the *tbl10* mutants possess normal trichomes.

The *tbl10* mutants exhibited enhanced drought resistance

Some pectin mutants have been shown to be compromised in their abiotic stress tolerance although none of the studies have specifically addressed pectin acetylation (Chen *et al.*, 2005; Keppler and Showalter, 2010; Levesque-Tremblay *et al.*, 2015). Therefore, it was of interest to investigate the drought response of the *tbl10* mutants. When the plants were exposed to severe drought stress (no watering for 15 days), we observed a significant increase of survival in both *tbl10* mutants compared to wild type (Figure 8). After 2 days of rewatering, only 33% of wild-type plants recovered whereas 62 and 80% of *tbl10-1* and *tbl10-2* plants recovered, respectively.

DISCUSSION

In the present study, we have isolated two independent homozygous mutant lines of *Arabidopsis* (*tbl10-1* and *tbl10-2*) (Figure 1). The *TBL10* transcript was abundant in leaves and scarce in stems (Figure 1c), which corresponded with the promoter activity of *TBL10* *in planta* (Figure 2). The *tbl10* mutants were shown to possess significantly lower levels of alkali-labile acetyl esters as compared to the wild type in AIR derived from leaves, while no significant difference was detectable in stems (Figure 3). Analysis of pectin-enriched and pectin-depleted

fractions showed that the level of acetylation was reduced in the leaves but not in stems (Figure 4). Further analysis showed significant reduction in the degree of acetylation in the isolated RG-I but not in the isolated HG following enzymatic hydrolysis (Figure 5). Analysis of XyG by MALDI-TOF-MS and of mannan and xylan by HSQC 2D-NMR experiments showed no significant difference between the *tbl10* mutants and the wild type (Figure 6, S4). Taken together, these results indicate that *TBL10* is required for *O*-acetylation of RG-I. Generally, based on available evidence so far, the large family of TBL proteins have relatively narrow substrate specificities, unlike for example the much smaller family of RWA proteins, which clearly overlap in which polysaccharides they affect. Nevertheless, we cannot exclude that *TBL10* may have some activity in acetylation of other polysaccharides; but, if it does, any such activity would be redundant with other acetyltransferases. Indeed, other TBL proteins involved in acetylation of XyG, xylan and mannan have already been reported (Gille *et al.*, 2011; Lee *et al.*, 2011; Yuan *et al.*, 2013, 2016a,b,c; Urbanowicz *et al.*, 2014; Gao *et al.*, 2017). The isolated HG from the *tbl10* mutants showed no change in acetylation, suggesting that HG is predominantly or exclusively acetylated by other as yet unidentified enzymes.

TBL10 is the first member of the TBL family proteins that is shown to be involved in *O*-acetylation of RG-I. Prior to this study, nine TBLs had been functionally assigned to *O*-acetylation of hemicelluloses and all of them belong to

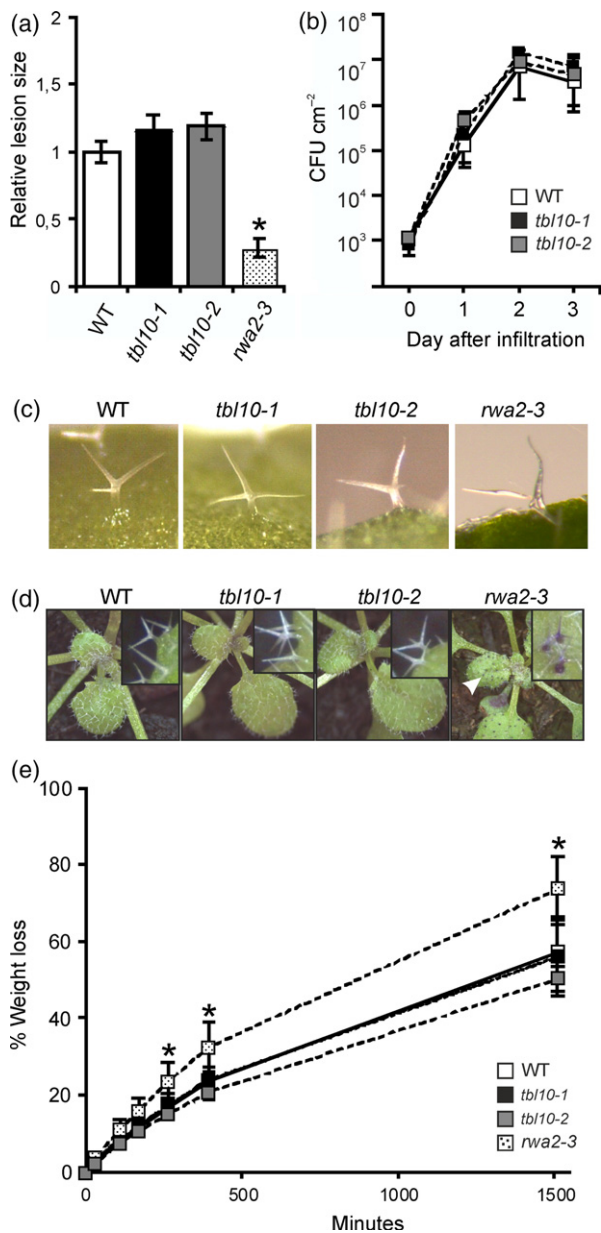


Figure 7. Phenotypic analysis of the wild type, the *tbl10* mutants, and the *rwa2-3* mutant of Arabidopsis.

(a) Disease development upon infection by *B. cinerea* based on at least 28 independent biological samples for each genotype. Error bars indicate standard errors. (b) Growth of *P. syringae* pv. tomato DC3000 in leaves, based on 6 independent biological samples for each genotype. Error bars indicate standard deviations. (c) Bright-field images of trichomes on leaves. Representative images are shown. (d) Toluidine blue staining of trichomes in leaves. Representative images are shown. The white arrowhead points at an example of staining. Close-up images of trichomes are shown in inserts. (e) Water loss kinetics in detached rosette leaves, based on four independent biological replicates. Error bars indicate standard deviation. Statistically significant differences, as assessed by Student's *t*-test ($P < 0.05$), are indicated by asterisks (*). Only *rwa2-3* showed significant differences in panel (a) and (e). [Colour figure can be viewed at wileyonlinelibrary.com].

Clusters IV and V in the TBL phylogenetic tree (Figure S1). TBL10 belongs to Cluster I, to which TBR also belongs. It was recently shown that *tbr* mutants have a reduced level

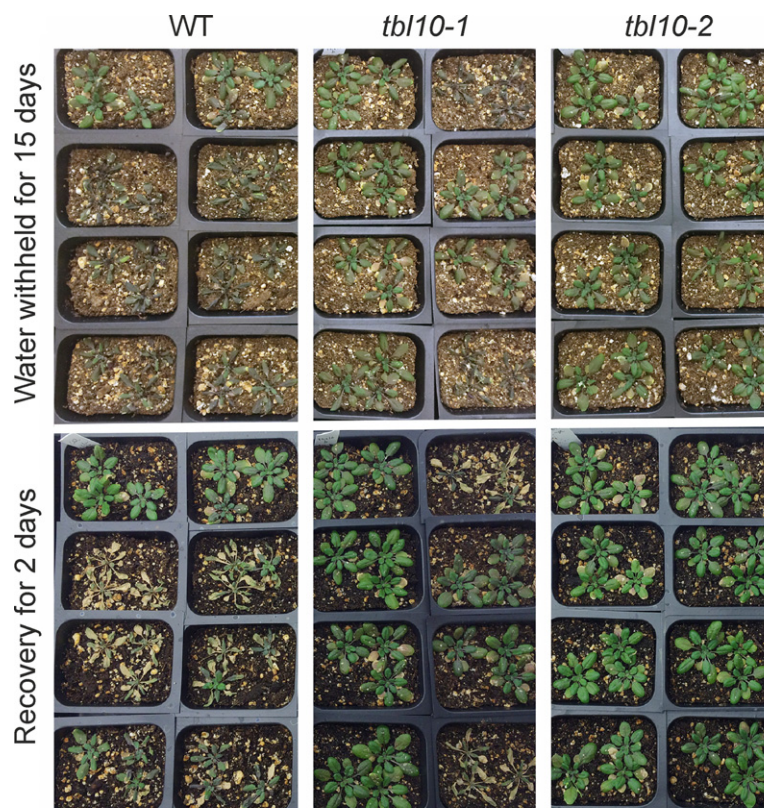
of *O*-acetylation in pectins, although the exact class of pectins affected by *tbr* remains unknown (Sinclair *et al.*, 2017). Nevertheless, we propose that TBL family proteins belonging to Cluster I, and possibly Cluster II, are involved in *O*-acetylation of pectins. It is plausible that TBL10 functions as an acetyltransferase transferring an acetyl group to the RG-I backbone, given the other TBL family proteins, notably TBL29, have been shown to be acetyltransferases. It is also possible that TBL10 has other molecular functions during *O*-acetylation of RG-I. For instance, it has recently been proposed that AX19, which possess limited sequence homology with TBL family proteins, is involved in acetylation of xylan and acts to produce an acetylated intermediate that is part of the *O*-acetylation pathway (Schultink *et al.*, 2015).

While TBR might also play roles in *O*-acetylation of pectins, there are notable differences between TBR and TBL10 with respect to their potential biological functions *in planta*. Firstly, tissue-wide expression patterns of the *TBR* and *TBL10* transcripts are markedly different. The promoter activity of *TBR* was prominent in vasculature and trichomes (Bischoff *et al.*, 2010), whereas that of *TBL10* was observed both in vascular and non-vascular leaf tissues but not in trichomes (Figure 2,S2). Moreover, *TBR* was found to be co-expressed with genes encoding components in cellulose synthesis (*CESA3*, *CESA5*, *CESA6*, *POM/CTL1*, *COBRA*) (Bischoff *et al.*, 2010), whereas *TBL10* does not appear to have a notable correlation with genes involved in cellulose synthesis based on ATTED-II (Obayashi *et al.*, 2011). Secondly, the *tbr* mutant exhibited fragile and collapsed trichomes (Potikha and Delmer, 1995; Bischoff *et al.*, 2010; Suo *et al.*, 2013), whereas the *tbl10* mutants have morphologically normal trichomes (Figure 7). We have previously proposed that decreased *O*-acetylation of pectins causes collapsed trichomes (Nafisi *et al.*, 2015). These observations suggest that TBR and TBL10 are differently involved in *O*-acetylation, possibly targeting different pectic classes (e.g. HG or RG-I) in different tissues, thereby impacting the plant physiology differently.

Previously, *in-muro* overexpression of a pectin acetyltransferase (PAE1), presumably targeting *O*-acetylation of HG, in tobacco (*Nicotiana tabacum*) led to wrinkled leaves (Gou *et al.*, 2012). Another study has shown that *in-muro* overexpression of an RGAE from *A. nidulans* in Arabidopsis increased the resistance of the transgenic plants towards *B. cinerea* (Pogorelko *et al.*, 2013). Notably, the *tbl10* mutants appeared normal and no sign of wrinkling was observed (Figures 2 and 7). Furthermore, the *tbl10* mutants exhibited the wild-type level of susceptibility to this fungal pathogen (Figure 7). How could the different deacetylation mutants lead to different phenotypic outcomes? It should be noted that proteins annotated as RGAE can exhibit mixed substrate preferences. For

Figure 8. Drought response of wild type and the *tbl10* mutants.

Forty-five plants of each genotype were grown for 3 weeks and then subjected to severe drought by withholding water for 14 days. Subsequently, the plants were re-watered and the number of green, surviving plants was determined after 2 days. The experiment was repeated twice with similar results. The data was analyzed with Chi-square test and both *tbl10-1* and *tbl10-2* showed better survival than wild type ($P < 0.01$ and $P < 0.001$, respectively). [Colour figure can be viewed at wileyonlinelibrary.com].



No. of plants	WT	<i>tbl10-1</i>	<i>tbl10-2</i>
Recovery	15	28	36
No recovery	30	17	9
χ^2		6.9	21.9
<i>P</i> value		<0.01	<0.001

*Degree of freedom of 1

instance a RGAE from *Aspergillus aculeatus* specifically removes acetyl groups bound to GalA residues in RG-I (Searle-van Leeuwen *et al.*, 1992), whereas another RGAE, also from *A. aculeatus*, can deacetylate both HG and RG-I (Bonnin *et al.*, 2008). This ambiguity is further highlighted in a recent study, wherein a previously annotated RGAE in *Bacillus licheniformis* was found to confer acetyltransferase activity specific to the acetyl group attached to the *O*-3 position in GalA of HG (Remoroza *et al.*, 2014). Moreover, the RGAE transgenic plants also contained reduced amounts of *O*-acetylation in XyG (Pogorelko *et al.*, 2013), making assignments of specific *O*-acetylated polysaccharides to defined biological functions challenging. Nevertheless, given that the *tbl10* mutants defective in RG-I *O*-acetylation did not exhibit collapsed trichomes or altered disease susceptibility to *B. cinerea*, neither did the *tbl27/axy4-3* mutant (Nafisi *et al.*, 2015), the possibility that

deacetylation of RG-I or XyG being responsible for these phenotypes is unlikely. We hypothesize that deacetylation of HG is more likely to be the underlining cause of collapsed trichomes and increased disease resistance against *B. cinerea*.

The increased survival in response to severe drought in the *tbl10* mutants is an interesting observation although we cannot presently provide an explanation for this phenotype. Some cell wall mutants may show activation of drought defense responses in the absence of exogenous stress, for example this has been described for the *eskimo1* mutant deficient in TBL29 (Lefebvre *et al.*, 2011). However, this appears not to be the case with the *tbl10* mutants, which do not show any changes in growth and development or difference in water loss prior to the exogenous stress (Figure 7e). Interestingly, the *TBL10* promoter was active in vascular tissues and stomata (Figure 2), which

may suggest that *TBL10*, and hence acetylated RG-I, play roles in water uptake and transport.

Identification of genes involved in pectin *O*-acetylation is an important step towards understanding the biological and molecular functions of *O*-acetylation in various pectic molecules. In this study, we presented the case wherein *O*-acetylation in RG-I could be specifically reduced *in planta* and propose that TBLs in Cluster I, and possibly Cluster II, may function in *O*-acetylation of pectins.

EXPERIMENTAL PROCEDURES

Growth conditions of Arabidopsis plants and isolation T-DNA insertional lines

Arabidopsis plants were grown in chambers (Percival Scientific, Perry, IA, USA) at 20°C with 70% relative humidity with photoperiod of 12-h day and 12-h night at a light intensity of $\sim 120 \mu\text{mol m}^{-2} \text{sec}^{-1}$. Two homozygous T-DNA insertion lines in At3g06080 (*TBL10*), Salk_005890C (*tbl10-1*) and Salk_011296 (*tbl10-2*), were obtained from the Arabidopsis Biological Resource Center (abrc.osu.edu). Genotyping was done using gene- and T-DNA-specific primer sequences obtained from the T-DNA Primer Design tool provided by the Salk Institute Genomic Analysis Laboratory (<http://signal.salk.edu/tdnprimers.2.html>); primer sequences are listed in Table S1.

Pathogen infection assays

Detached leaves of 3 to 4-week old plants were inoculated with *Botrytis cinerea* strain IK2018 spore solution (5×10^5 spores ml^{-1} in half strength potato dextrose broth) as previously described (Nafisi *et al.*, 2015). To quantify lesion sizes, high quality digital images were acquired and processed with ImageJ (<https://imagej.nih.gov/ij/>). Treatments with *Pseudomonas syringae* DC3000 were performed as previously described (Rautengarten *et al.*, 2012). Briefly, leaves were infiltrated with diluted suspensions of *P. syringae* DC3000 (10^6 cells ml^{-1}) in 10 mM MgCl_2 . Four leaves were harvested from each genotype at each time point and the surface was sterilized in 70% (v/v) ethanol. The bacterial growth inside the leaves was enumerated by direct counting of the bacterial colonies in nutrient yeast glycerol medium containing 25 mg ml^{-1} rifampicin.

Drought stress assay

Seeds were surface sterilized and sown on solid medium containing 0.5× Murashige and Skoog salts including vitamins (1/2 MS medium) (Sigma-Aldrich, Søborg, Denmark) and 2% (w/v) sucrose. Following stratification (48 h, 4°C, in the dark), plates were transferred to a growth room (22°C, 100–200 $\mu\text{mol m}^{-2} \text{sec}^{-1}$, 14-h day and 10-h night). One-week-old seedlings were transferred to soil for 2 weeks under the same growth conditions and then subjected to progressive drought by withholding water for 14 days. The plants were re-watered and the number of surviving, green plants was counted after 2 days.

RNA extraction and RT-PCR

Plant materials frozen in liquid nitrogen were ground with a pestle and mRNA extracted using the RNeasy Plant Mini Kit (Qiagen, Vedbæk, Denmark) with on-column DNase treatment according to the manufacturer's instruction. The integrity of the RNA was confirmed by gel electrophoresis. Before cDNA synthesis, mRNA

concentrations were quantified by NanoDrop (ThermoFisher Scientific, Roskilde, Denmark) and normalized to the equal amounts. cDNA was synthesized using the iScript cDNA synthesis kit (Bio-Rad, Copenhagen, Denmark) according to the manufacturer's protocol. Presence of the *TBL10* transcript in the wild type, *tbl10-1*, and *tbl10-2* was analyzed by using intron-spanning primers listed in Table S1, while *ACTIN2* (*ACT2*, AT3G18780) was used as a reference gene.

Expression analysis of the *TBL10* promoter using a *GUS* reporter

An 1800 kb 5' upstream sequence of the *TBL10* gene not including the start codon was amplified by PCR using USER compatible primers (Nour-Eldin *et al.*, 2010) listed in Table S1. The promoter sequence was inserted in the pLIFE41vector, containing the *BAR* gene conferring resistance to BASTA (Bayer CropScience, Copenhagen, Denmark) within the T-DNA cassette. The resulting vector was introduced to *Agrobacterium tumefaciens* via electroporation. Arabidopsis wild-type plants were transformed by floral dipping and selection after two consecutive spraying with BASTA following the manufacturer's instruction. The presence of the *TBL10*-promoter::*GUS* construct was verified by PCR with the primers listed in Table S1. Leaves, stems and roots from 6-week-old transgenic plants were examined for GUS activity after incubating for overnight (16 h) at 25°C in a GUS staining solution consisting of 50 mM sodium phosphate buffer, pH 7.0, 10 mM ethylenediaminetetraacetic acid, 0.1% (v/v) Triton X-100, 0.5 mM potassium ferricyanide, 0.5 mM potassium ferrocyanide, and 1 mg ml^{-1} 5-bromo-4-chloro-3-indolyl- β -D-glucuronide. Under these conditions, the staining was not saturating. For saturating staining, incubation at 37°C was performed. Chlorophylls were extracted with 96% (v/v) ethanol. Initial screening for GUS expression was performed using 22 independent transgenic plants, and subsequently 5 independent T2 plants were analyzed in detail.

AIR preparation

AIR was prepared following previously described procedures with some modifications (Fry, 1988; Harholt *et al.*, 2006). Leaf and stem materials were harvested in liquid nitrogen, ground to a fine powder in a mixer mill (Retsch, Haan, Germany) and suspended in ice-cold 96% (v/v) ethanol. The samples were placed on glass microfiber filters (GE Healthcare Europe GmbH, Brøndby, Denmark) and washed several times in 96% (v/v) ethanol until free of chlorophyll and finally washed in 100% (v/v) acetone and left to dry over night at room temperature. To remove starch, dried AIR was ground again in the Retch mixer mill and suspended in a pre-heated (at $\sim 90^\circ\text{C}$) destarching buffer consisting of 10 mM potassium phosphate buffer, pH 6.5, 1 mM CaCl_2 and 0.05% (w/v) sodium azide. One hundred milligrams of AIR were resuspended in 25 mL of the destarching buffer and were allowed to gelatinize for 30 sec before addition of 1 U ml^{-1} thermostable α -amylase (Megazyme, Wicklow, Ireland) followed by incubation at 85°C for 15 min. The samples were cooled to room temperature and 1 U ml^{-1} each of amyloglucosidase and pullulanase (Megazyme) was added. The mixtures were incubated for 16 h at room temperature with gentle shaking. Destarched AIR was collected by centrifugation at 21 000× *g* for 10 min and pellets were washed with destarching buffer on glass microfiber filters (GE Healthcare Europe GmbH), rinsed in water, and dried overnight.

Fractionation of AIR

Pectin-enriched and pectin-depleted fractions were obtained by incubating destarched AIR in a digesting buffer consisting of

50 mM cyclohexane diamine tetraacetic acid, 50 mM ammonium formate, and 0.05% (w/v) sodium azide. Six U ml⁻¹ of ePG from *Aspergillus aculeatus* (Megazyme) and 4 U ml⁻¹ of PME (Novozymes, Bagsværd, Denmark) were added to the solution followed by a 24-h incubation with gentle shaking. After incubation, the enzymes were inactivated at 95°C for 10 min, and the reactions were allowed to cool to room temperature before centrifugation at 21 000× g for 10 min at room temperature. The supernatants containing the released pectins were transferred to new tubes. The remaining pellets containing hemicelluloses and residual pectin were washed twice with the digestion buffer and resuspended in 1 ml digestion buffer. Acetic acid content from these fractions was determined colorimetrically using an enzyme-coupled assay or by reverse-phase high-pressure liquid chromatography (HPLC) as detailed below. HG and RG-I were isolated from destarched AIR treated with ePG and PME, as described above. Following enzymatic treatment, hydrolysates were filtered through nylon membranes with a pore size of 0.45 µm (VWR International, Søborg, Denmark) and concentrated by Amicon Ultra spin filters with a molecular-weight-cut-off of 10 kDa (Sigma-Aldrich). The flow-throughs, consisting of HG-derived small molecular weight products, were recovered as the HG fraction, while the concentrated materials in the spin filters were subjected to size exclusion chromatography (Superdex 200 10/300 GL column) using 50 mM ammonium formate (pH 5.0) as eluent as previously described (Stonebloom *et al.*, 2016). The refraction index was used to monitor carbohydrates in eluents as described previously. The HG and RG-I fractions were analyzed for sugar composition of non-cellulosic polysaccharides and acetic acid content as described below. At least three independent biological replicates were analyzed for each genotype. Values are expressed as relative percentage and are the means ± standard deviations (SD).

Quantification of acetic acid

To release acetic acid from a sample, 100 µl of the sample were incubated with 100 µl of 1 M NaOH for 1 h followed by neutralization by the addition of 100 µl of 1 M HCl. The amount of released acetic acid was determined using spectrophotometric procedures using a standard curve of acetic acid to calculate concentrations using an enzyme-coupled assay (Megazyme). Alternatively, the acetic acid content was measured by using reverse-phase HPLC. The samples were passed through 0.22 µm Hydrophilic, Low Protein Binding Durapore Membrane (Merck Millipore, Hellerup, Denmark) and the filtrates were injected into a Shimadzu chromatographer LC-20AD equipped with a SIL-20AC HT autosampler, UV detector SPD-M20A, and a reverse phase column (00G-4375-E0, Phenomenex, Værløse, Denmark). Samples were eluted at a flow rate of 0.7 ml min⁻¹ in 20 mM potassium phosphate buffer, adjusted to pH 2.9 with 85% (v/v) phosphoric acid. The eluents were detected at 220 nm with a diode array detector. Three independent biological replicates were analyzed for each genotype. Values are expressed as relative percentage and are the means ± SD.

Monosaccharide composition analysis

Destarched AIR (10 mg) or purified HG and RG-I fractions were incubated in 1 ml of 2 M TFA for 1 h at 120°C. The samples were allowed to cool to room temperature and TFA was evaporated under vacuum and resuspended in 1 ml of distilled water. The samples were filtered as described above, and analyzed by high-performance anion exchange chromatography with pulsed amperometric detection (HPAEC-PAD), using a PA20 column (ThermoFisher Scientific). The program settings were as previously described (Øbro *et al.*, 2004). Three independent biological

replicates were analyzed for each genotype. Values are expressed as relative percentage and are the means ± SD.

MALDI-TOF analysis

XyG oligosaccharides were obtained as previously reported with slight modifications (Dardelle *et al.*, 2010). Briefly, the pectin-depleted fractions (5 mg) were incubated overnight at 37°C under agitation at 180 rpm in 500 µl of *endo*-(1–4)-β-D-glucanase (10 U, EC 3.2.1.4; Megazyme) prepared in 10 mM sodium acetate buffer, pH 5. After the addition of 2 ml of 96% (v/v) ethanol, samples were precipitated overnight at –20°C and centrifuged for 10 min at 10 000× g. Supernatants were evaporated under a flow of air to concentrate the XyG oligomers. XyG from tamarind seeds (Megazyme) was treated similarly and used as a control.

A voyager DE-Pro matrix-assisted laser desorption ionization-time of flight (MALDI-TOF) mass spectrometer (Applied Biosystems, Foster City, CA, USA) equipped with a 337-nm nitrogen laser was used to analyze XyG fragments. Mass spectra were collected in the reflector delayed extraction mode using 2,5-dihydroxybenzoic acid (Sigma-Aldrich) as matrix. The matrix, freshly dissolved at 5 mg ml⁻¹ in a solution composed of 70:30 acetonitrile/0.1% (v/v) TFA, was mixed with the water-solubilized oligosaccharides in a ratio 1:1 (v/v). The spectra were recorded in a positive mode, using an acceleration voltage of 20 000 V with a delay time of 100 ns and above 50% of the laser energy. They were externally calibrated using commercially available mixtures of peptides and proteins (ProteoMass™ MALDI Calibration Kit, Sigma-Aldrich). Laser shots were accumulated for each spectrum to obtain an acceptable signal to noise ratio (sum of three spectra of 1000 shots per spectrum). Four independent biological replicates were analyzed for each genotype. Values are expressed as relative percentage and are the means ± SD.

ACCESSION NUMBERS

The *TBL10* gene has the ID At3g06080.

ACKNOWLEDGEMENTS

The authors wish to thank Dr. Jozef Mravec (University of Copenhagen) for assistance with microscopy and Yuuri Tsuboi and Tomoko Matsumoto (RIKEN) for technical assistance with NMR analysis. This work was supported by the Innovation Foundation Denmark [Biomass for the 21st century, grant number 001-2011-4], Villum Fonden [project no. 13363] and the DOE Joint BioEnergy Institute (<http://www.jbei.org>) was supported by the U. S. Department of Energy, Office of Science, Office of Biological and Environmental Research, through contract DE-AC02-05CH11231 between Lawrence Berkeley National Laboratory and the U. S. Department of Energy. YR and JY were supported by China Scholarship Council.

CONFLICT OF INTEREST

The authors declare no conflicts of interest related to this research.

SUPPORTING INFORMATION

Additional Supporting Information may be found in the online version of this article.

Figure S1. A phylogenetic tree based on 46 TBL proteins in Arabidopsis.

Figure S2. Expression level of *TBL10* in various tissues in Arabidopsis.

Figure S3. Monosaccharide composition of pectin-enriched and pectin-depleted fractions derived from leaves of the wild type and *tbl10* mutants of Arabidopsis.

Figure S4. Monosaccharide compositions of RG-I and HG fractions isolated from leaves of Arabidopsis wild type and *tbl10-1* mutant.

Figure S5. Comparison of expanded HSQC 2D-NMR spectra of wild-type and *tbl10-2* mutant of Arabidopsis leaf cell-walls solubilized in DMSO-[Emim]Ac.

Figure S6. Morphological analysis of stem sections of the wild type and the *tbl10* mutants of Arabidopsis.

Table S1. List of primers.

Methods S1. NMR analyses for cell-wall components.

Methods S2. Stem sectioning, staining and microscopy.

REFERENCES

- Alvarez-Buylla, E.R., Benítez, M., Corvera-Poiré, A. et al. (2010) Flower development. *Arabidopsis Book*, 8, e0127.
- Atmodjo, M.A., Hao, Z. and Mohnen, D. (2013) Evolving views of pectin biosynthesis. *Annu. Rev. Plant Biol.* **64**, 747–779.
- Bischoff, V., Nita, S., Neumetzler, L., Schindelasch, D., Urbain, A., Eshed, R., Persson, S., Delmer, D. and Scheible, W.R. (2010) TRICHOME BIREFRINGENCE and its homolog AT5G01360 encode plant-specific DUF231 proteins required for cellulose biosynthesis in Arabidopsis. *Plant Physiol.* **153**, 590–602.
- Bonnin, E., Clavurier, K., Daniel, S., Kauppinen, S., Mikkelsen, J.D.M. and Thibault, J.-F. (2008) Pectin acetyltransferases from *Aspergillus* are able to deacetylate homogalacturonan as well as rhamnogalacturonan. *Carbohydr. Polym.* **74**, 411–418.
- Busse-Wicher, M., Gomes, T.C., Tryfona, T., Nikolovski, N., Stott, K., Grantham, N.J., Bolam, D.N., Skaf, M.S. and Dupree, P. (2014) The pattern of xylan acetylation suggests xylan may interact with cellulose microfibrils as a twofold helical screw in the secondary plant cell wall of Arabidopsis thaliana. *Plant J.* **79**, 492–506.
- Carpita, N. (2015) Cell walls: structure, formation, and expansion. In *Plant Physiology and Development* (Taiz, L., Zeiger, E., Møller, I. M. and Murphy, A., eds). Massachusetts: Sinauer Associates Inc, pp. 380–405.
- Chen, Z., Hong, X., Zhang, H., Wang, Y., Li, X., Zhu, J.-K. and Gong, Z. (2005) Disruption of the cellulose synthase gene, *AtCesA8/IRX1*, enhances drought and osmotic stress tolerance in Arabidopsis. *Plant J.* **43**, 273–283.
- Cheng, K., Sorek, H., Zimmermann, H., Wemmer, D.E. and Pauly, M. (2013) Solution-state 2D NMR spectroscopy of plant cell walls enabled by a dimethylsulfoxide-d₆/1-ethyl-3-methylimidazolium acetate solvent. *Anal. Chem.* **85**, 3213–3221.
- Dardelle, F., Lehner, A., Ramdani, Y., Bardor, M., Lerouge, P., Driouch, A. and Mollet, J.C. (2010) Biochemical and immunocytological characterizations of Arabidopsis pollen tube cell wall. *Plant Physiol.* **153**, 1563–1576.
- Fry, S.C. (1988) *The Growing Plant Cell Wall: Chemical and Metabolic Analysis*. Essex, UK: Longman Scientific and Technical.
- Fry, S.C., Aldington, S., Hetherington, P.R. and Aitken, J. (1993) Oligosaccharides as signals and substrates in the plant cell wall. *Plant Physiol.* **103**, 1–5.
- Gao, Y., He, C., Zhang, D. et al. (2017) Two trichome birefringence-like proteins mediate xylan acetylation, which is essential for leaf blight resistance in rice. *Plant Physiol.* **173**, 470–481.
- Gille, S., de Souza, A., Xiong, G.Y., Benz, M., Cheng, K., Schultink, A., Reza, I.B. and Pauly, M. (2011) O-acetylation of Arabidopsis hemicellulose xyloglucan requires *AXY4* or *AXY4L*, proteins with a TBL and DUF231 domain. *Plant Cell*, **23**, 4041–4053.
- Gonçalves, V.M.F., Evtuguin, D.V. and Domingues, M.R.M. (2008) Structural characterization of the acetylated heteroxylan from the natural hybrid *Paulownia elongata*/*Paulownia fortunei*. *Carbohydr. Res.* **343**, 256–266.
- Gou, J.Y., Miller, L.M., Hou, G., Yu, X.H., Chen, X.Y. and Liu, C.J. (2012) Acetyltransferase-mediated deacetylation of pectin impairs cell elongation, pollen germination, and plant reproduction. *Plant Cell*, **24**, 50–65.
- Harholt, J., Jensen, J.K., Sørensen, S.O., Orfila, C., Pauly, M. and Scheller, H.V. (2006) ARABINAN DEFICIENT 1 is a putative arabinosyltransferase involved in biosynthesis of pectic arabinan in Arabidopsis. *Plant Physiol.* **140**, 49–58.
- Ishii, T. (1991) Acetylation at O-2 of arabinofuranose residues in feruloylated arabinoxylan from bamboo shoot cell-walls. *Phytochemistry*, **30**, 2317–2320.
- Ishii, T. (1997) O-acetylated oligosaccharides from pectins of potato tuber cell walls. *Plant Physiol.* **113**, 1265–1272.
- Keppeler, B.D. and Showalter, A.M. (2010) IRX14 and IRX14-LIKE, two glycosyl transferases involved in glucuronoxylan biosynthesis and drought tolerance in Arabidopsis. *Mol. Plant*, **3**, 834–841.
- Lee, C., Teng, Q., Zhong, R. and Ye, Z.H. (2011) The four Arabidopsis reduced wall acetylation genes are expressed in secondary wall-containing cells and required for the acetylation of xylan. *Plant Cell Physiol.* **52**, 1289–1301.
- Lefebvre, V., Fortabat, M.N., Ducamp, A., North, H.M., Maia-Grondard, A., Trouverie, J., Boursiac, Y., Mouille, G. and Durand-Tardif, M. (2011) ESKIMO1 disruption in Arabidopsis alters vascular tissue and impairs water transport. *PLoS One*, **6**, e16645.
- Lerouge, P., O'Neill, M.A., Darvill, A.G. and Albersheim, P. (1993) Structural characterization of endo-glycanase-generated oligoglycosyl side chains of rhamnogalacturonan I. *Carbohydr. Res.* **243**, 359–371.
- Levesque-Tremblay, G., Pelloux, J., Braybrook, S.A. and Müller, K. (2015) Tuning of pectin methylesterification: consequences for cell wall biomechanics and development. *Planta*, **242**, 791–811.
- Liners, F., Gaspar, T. and Cutsem, P.Van (1994) Acetyl- and methyl-esterification of pectins of friable and compact sugar-beet calli: consequences for intercellular adhesion. *Planta*, **192**, 545–556.
- Lundqvist, J., Teleman, A., Junel, L., Zacchi, G., Dahlman, O., Tjerneld, F. and Stålbrand, H. (2002) Isolation and characterization of galactoglucomannan from spruce (*Picea abies*). *Carbohydr. Polym.* **48**, 29–39.
- Manabe, Y., Nafisi, M., Verhertbruggen, Y. et al. (2011) Loss-of-function mutation of REDUCED WALL ACETYLATION2 in Arabidopsis leads to reduced cell wall acetylation and increased resistance to *Botrytis cinerea*. *Plant Physiol.* **155**, 1068–1078.
- Manabe, Y., Verhertbruggen, Y., Gille, S. et al. (2013) Reduced wall acetylation proteins play vital and distinct roles in cell wall O-acetylation in Arabidopsis. *Plant Physiol.* **163**, 1107–1117.
- Manna, S. and McAnalley, B.H. (1993) Determination of the position of the O-acetyl group in a β -(1 \rightarrow 4)-mannan (acemannan) from *Aloe barbadensis* Miller. *Carbohydr. Res.* **241**, 317–319.
- Mohnen, D. (2008) Pectin structure and biosynthesis. *Curr. Opin. Plant Biol.* **11**, 266–277.
- Nafisi, M., Stranne, M., Fimognari, L. et al. (2015) Acetylation of cell wall is required for structural integrity of the leaf surface and exerts a global impact on plant stress responses. *Front. Plant Sci.* **6**, 550.
- Nour-Eldin, H.H., Geu-Flores, F. and Halkier, B.A. (2010) USER cloning and USER fusion: the ideal cloning techniques for small and big laboratories. *Methods Mol. Biol.* **643**, 185–200.
- Nunes, F.M., Domingues, M.R. and Coimbra, M.A. (2005) Arabinosyl and glucosyl residues as structural features of acetylated galactomannans from green and roasted coffee infusions. *Carbohydr. Res.* **340**, 1689–1698.
- Obayashi, T., Nishida, K., Kasahara, K. and Kinoshita, K. (2011) ATTED-II updates: condition-specific gene coexpression to extend coexpression analyses and applications to a broad range of flowering plants. *Plant Cell Physiol.* **52**, 213–219.
- Øbro, J., Harholt, J., Scheller, H.V. and Orfila, C. (2004) Rhamnogalacturonan I in *Solanum tuberosum* tubers contains complex arabinogalactan structures. *Phytochemistry*, **65**, 1429–1438.
- Orfila, C., Degan, F., Jørgensen, B., Scheller, H., Ray, P. and Ulvskov, P. (2012) Expression of mung bean pectin acetyl esterase in potato tubers: effect on acetylation of cell wall polymers and tuber mechanical properties. *Planta*, **236**, 185–196.
- Pabst, M., Fischl, R.M., Brecker, L., Morelle, W., Fauland, A., Köfeler, H., Altmann, F. and Léonard, R. (2013) Rhamnogalacturonan-II structure shows variation in the side chains monosaccharide composition and methylation status within and across different plant species. *Plant J.* **76**, 61–72.
- Pauly, M. and Scheller, H.V. (2000) O-acetylation of plant cell wall polysaccharides: identification and partial characterization of a

- rhamnogalacturonan O-acetyl-transferase from potato suspension-cultured cells. *Planta*, **210**, 659–667.
- Perrone, P., Hewage, C.M., Thomson, A.R., Bailey, K., Sadler, I.H. and Fry, S.C.** (2002) Patterns of methyl and O-acetyl esterification in spinach pectins: new complexity. *Phytochemistry*, **60**, 67–77.
- Petersen, T.N., Brunak, S., von Heijne, G. and Nielsen, H.** (2011) SignalP 4.0: discriminating signal peptides from transmembrane regions. *Nat. Methods*, **8**, 785–786.
- Pogorelko, G., Lionetti, V., Fursova, O., Sundaram, R.M., Qi, M., Whitham, S.A., Bogdanove, A.J., Bellincampi, D. and Zabolina, O.A.** (2013) Arabidopsis and *Brachypodium distachyon* transgenic plants expressing *Aspergillus nidulans* acetyltransferases have decreased degree of polysaccharide acetylation and increased resistance to pathogens. *Plant Physiol.* **162**, 9–23.
- Potikha, T. and Delmer, D.P.** (1995) A mutant of *Arabidopsis thaliana* displaying altered patterns of cellulose deposition. *Plant J.* **7**, 453–460.
- Rautengarten, C., Ebert, B., Ouellet, M. et al.** (2012) Arabidopsis deficient in cutin ferulate encodes a transferase required for feruloylation of omega-hydroxy fatty acids in cutin polyester. *Plant Physiol.* **158**, 654–665.
- Remoroza, C., Wagenknecht, M., Gu, F., Buchholt, H.C., Moerschbacher, B.M., Schols, H.A. and Gruppen, H.** (2014) A *Bacillus licheniformis* pectin acetyltransferase is specific for homogalacturonans acetylated at O-3. *Carbohydr. Polym.* **107**, 85–93.
- Ridley, B.L., O'Neill, M.A. and Mohnen, D.** (2001) Pectins: structure, biosynthesis, and oligogalacturonide-related signaling. *Phytochemistry*, **57**, 929–967.
- Scheller, H.V. and Ulvskov, P.** (2010) Hemicelluloses. *Annu. Rev. Plant Biol.* **61**, 263–289.
- Schultink, A., Naylor, D., Dama, M. and Pauly, M.** (2015) The role of the plant-specific ALTERED XYLOGLUCAN9 protein in Arabidopsis cell wall polysaccharide O-acetylation. *Plant Physiol.* **167**, 1271–1283.
- Schwacke, R., Schneider, A., van der Graaff, E. et al.** (2003) ARAMEMNON, a novel database for Arabidopsis integral membrane proteins. *Plant Physiol.* **131**, 16–26.
- Searle-van Leeuwen, M.J.F., van den Broek, L.A.M., Schols, H.A., Beldman, G. and Voragen, A.G.J.** (1992) Rhamnogalacturonan acetyltransferase: a novel enzyme from *Aspergillus aculeatus*, specific for the deacetylation of hairy (ramified) regions of pectins. *Appl. Microbiol. Biotechnol.* **38**, 347–349.
- Sims, I.M., Munro, S.L.A., Currie, G., Craik, D. and Bacic, A.** (1996) Structural characterisation of xyloglucan secreted by suspension-cultured cells of *Nicotiana glauca*. *Carbohydr. Res.* **293**, 147–172.
- Sinclair, S.A., Larue, C., Bonk, L. et al.** (2017) Etiolated seedling development requires repression of photomorphogenesis by a small cell-wall-derived dark signal. *Curr. Biol.* **27**, 3403–3418.e7.
- Stonebloom, S., Ebert, B., Xiong, G. et al.** (2016) A DUF-246 family glycosyltransferase-like gene affects male fertility and the biosynthesis of pectic arabinogalactans. *BMC Plant Biol.* **16**, 90.
- Suo, B., Seifert, S. and Kirik, V.** (2013) Arabidopsis GLASSY HAIR genes promote trichome papillae development. *J. Exp. Bot.* **64**, 4981–4991.
- Tanaka, T., Tanaka, H., Machida, C., Watanabe, M. and Machida, Y.** (2004) A new method for rapid visualization of defects in leaf cuticle reveals five intrinsic patterns of surface defects in Arabidopsis. *Plant J.* **37**, 139–146.
- Urbanowicz, B.R., Peña, M.J., Moniz, H.A., Moremen, K.W. and York, W.S.** (2014) Two Arabidopsis proteins synthesize acetylated xylan in vitro. *Plant J.* **80**, 197–206.
- Vogel, J.P., Raab, T.K., Somerville, C.R. and Somerville, S.C.** (2004) Mutations in PMR5 result in powdery mildew resistance and altered cell wall composition. *Plant J.* **40**, 968–978.
- Vriesmann, L. and Petkowicz, C.** (2013) Highly acetylated pectin from cacao pod husks (*Theobroma cacao* L.) forms gel. *Food Hydrocoll.* **33**, 58–65.
- Whitcombe, A.J., Oneill, M.A., Steffan, W., Albersheim, P. and Darvill, A.G.** (1995) Structural characterization of the pectic polysaccharide, rhamnogalacturonan-II. *Carbohydr. Res.* **271**, 15–29.
- Winter, D., Vinegar, B., Nahal, H., Ammar, R., Wilson, G.V. and Provart, N.J.** (2007) An “electronic fluorescent pictograph” browser for exploring and analyzing large-scale biological data sets. *PLoS One*, **2**, 1–12.
- Xiong, G.Y., Cheng, K. and Pauly, M.** (2013) Xylan O-acetylation impacts xylem development and enzymatic recalcitrance as indicated by the Arabidopsis mutant tbl29. *Mol. Plant*, **6**, 1373–1375.
- York, W.S., Kolli, V.S.K., Orlando, R., Albersheim, P. and Darvill, A.G.** (1996) The structures of arabinoxyloglucans produced by solanaceous plants. *Carbohydr. Res.* **285**, 99–128.
- Yuan, Y., Teng, Q., Zhong, R. and Ye, Z.H.** (2013) The Arabidopsis DUF231 domain-containing protein ESK1 mediates 2-O- and 3-O-acetylation of xylosyl residues in xylan. *Plant Cell Physiol.* **54**, 1186–1199.
- Yuan, Y., Teng, Q., Zhong, R., Haghghat, M., Richardson, E.A. and Ye, Z.-H.** (2016a) Mutations of Arabidopsis TBL32 and TBL33 affect xylan acetylation and secondary wall deposition. *PLoS One*, **11**, e0146460.
- Yuan, Y., Teng, Q., Zhong, R. and Ye, Z.H.** (2016b) Roles of Arabidopsis TBL34 and TBL35 in xylan acetylation and plant growth. *Plant Sci.* **243**, 120–130.
- Yuan, Y., Teng, Q., Zhong, R. and Ye, Z.H.** (2016c) TBL3 and TBL31, two Arabidopsis DUF231 domain proteins, are required for 3-O-monoacetylation of xylan. *Plant Cell Physiol.* **57**, 35–45.